

MULTI-ANGULAR SCATTEROMETER MEASUREMENTS FOR VARIOUS STAGES OF RICE GROWTH

K.-S. Lim, V.-C. Koo, and H.-T. Ewe

Faculty of Engineering
Multimedia University
Persiaran Multimedia, 63100 Cyberjaya, Malaysia

Abstract—This paper presents comprehensive measurements of radar backscatter from rice crops using a ground-based 6 GHz C-band scatterometer system. The measurements were conducted over an entire season from the early vegetative stage of the plants to the ripening stage with full polarization combinations of HH, VV, HV and VH at the incident angle range from 0° to 60° . The objective of this paper is to assess the use of the ground-based scatterometer data for the investigation of temporal variation of different incident angle in the rice growth monitoring application. A further study on the angular response for different rice growth stages was also performed in order to have a better understanding of the backscattering behavior of the rice crops and therefore, monitoring of rice crops growth using operational scatterometer system.

1. INTRODUCTION

Recently, the need for management of the food supply is apparent owing to the ever increasing world population which has led to high demand of global food production. Among the major crop types in the world, rice constitutes the basic food for the people in many parts of Asia, as well as in Europe and America. Hence, there is a strong need for effective means to monitor rice crops in order to control and maintain a close balance between the rice production and demand.

Over the past few decades, there has been a considerable number of researchers who investigated the distribution of sources of the backscattering within vegetation canopies [1–24]. Field scatterometers were employed at 10 GHz (X-band) [7, 8], while other studies [15–20] used 4.75-GHz field scatterometers and the microwave scatterometer

C-band (MS-C). Investigation on the radar backscatter from the rice crops were done by Le Toan [25, 26] by using an airborne X-Band Synthetic Aperture Radar (SAR), VARAN-S, operating in HH and VV at the incident angle of 0° to 60° . On the other hand, Kurosu [27] had also conducted an experiment on the entire rice growth cycle with VV polarization at the incident angle of 23° while Kim [28] performed the measurements using X-band scatterometer. It appears from the literature that the radar backscattering coefficient varies with the measurement system used, and with the growth stage, due to the different physical structure of the rice plants. This variation may also be due to the difference in frequencies and incident angles. However, the number of observations in [25–27] was not sufficient to make a detailed comparison of the temporal variation of the backscattering coefficient while the experiment in [28] was limited to the short penetration depth of the X-band signal which may not be adequate for vegetation measurements where the size of the plant is larger than the wavelength. These reasons motivate the first investigation ever on the temporal behavior and the angular response of the radar backscattering from the rice crop fields throughout the entire growth season at C-band reported in this paper.

The paper is outlined as follows. Section 2 describes the design and configuration of the ground-based scatterometer with its detailed specification. The ground truth measurement procedure is also explained. This is followed by discussion on the experimental results in Section 3. In Section 4, we conclude and summarize this work.

2. GROUND-BASED SCATTEROMETER AND GROUND TRUTHS

A ground-based C-band scatterometer was constructed and installed on a mobile telescopic truck platform with the purpose of in-situ scattering measurements [29]. It was developed with inexpensive FM-CW radar at a center frequency of 6 GHz. Some modifications have been performed on the existing scatterometer particularly in the data acquisition unit for the improvement on the overall system stability and the data provision of dynamic range. For clutter cross-section measurements, the radar can be used to obtain N independent samples of the surface scattering coefficient within a single footprint, with N given by

$$N = \frac{\Delta R}{r_R} \quad (1)$$

where ΔR is the effective range resolution and r_R is the best possible range resolution. On the other hand, volume scattering can take place and more independent samples are contributed to a particular measurement.

In this paper, polarimetric calibration of the system was done using a 12 inch (30 cm) diameter metallic sphere. A dual polarized parabola antennas allows the system to conduct full polarization measurements and the antenna positioning system is designed to control the incident angle from 0° to 60° . The specifications of the scatterometer system are given in Table 1.

Table 1. Specifications of the ground-based C-band scatterometer system.

System Parameter	Specification
System Configuration	
Operating Frequency	6 GHz (C band)
Operating wavelength	5 cm
Sweep Bandwidth	400 MHz
Modulation Frequency	60 Hz
Polarization	HH, HV, VH, VV
Polarization Isolation	35 dB
Antenna Gain	35 dB
Antenna 3 dB Bandwidth	3°
Best Possible Range Resolution	0.375 m
Platform	Boom Truck
Platform Height	25 m (vertical)
Measurement Capability	
Transmit Power	10 dBm
Received Power	-15 dBm to -92 dBm
∂° Dynamic range	+20 dB to -40 dB
Measurement Range	20 to 100 m
Incident Angle Coverage θ	0° to 70°
Minimum signal to noise ratio SNR	10 dB
Effective range resolution	~ 1.8 m at $\theta = 45^\circ$ 4.5 m at $\theta = 60^\circ$

The understanding of rice growing conditions and cultural practices are crucial in order to retrieve rice crop parameters for rice monitoring. Thus, ground truth measurements for an entire rice crop season have been conducted from March 13 to May 27, 2008 at Sungai Burung, Selangor, Malaysia. Figure 1 shows a photograph of the ground-based scatterometer during the measurement. The seeds of the plants were spread randomly over the entire rice field and the variety used in this site was MR219. Figure 2 shows a photograph of the test site.

Parameters that were measured include plant geometry such as plant height, leaf length, leaf width, leaf thickness and tiller density, and their range of values are as shown in Table 2. These values have been averaged to give a general view of the physical structure of the plant. The measurements were done by a group of researchers from Multimedia University and the Malaysian Remote Sensing Agency (MACRES) as a collective effort for various research purposes.

Some of these parameters were not necessary for this work, but are given here for the sake of completeness and for the ongoing theoretical modeling efforts.

3. EXPERIMENTAL RESULTS AND DISCUSSION

In this paper, measurements have been conducted at full polarization with the incident angle ranging from 0° to 60° . The digitized time



Figure 1. Ground-based C-band scatterometer during measurement trip.

Table 2. The summary of the physical ground truth measurements.

Plant Age (day)	38	51	62	84	96	105
Plant Height (cm)	30.2	38.5	47.2	80.4	105.6	109.4
No.of Leaves per Stem	3	4	5	5	5	6
Leaf Length (cm)	15.96	25.8	36	49.4	38.2	51.2
Leaf Width (mm)	5.5	8.3	10.2	12	13.6	15.6
Leaf Thickness (mm)	0.19	0.2	0.2	0.17	0.25	0.3
Tiller Length (cm)	9.8	13.5	16.8	32.6	61.2	77.2
Tiller Diameter (mm)	4.6	9.8	9.8	11.2	11.2	11.4
Tiller Density (m^{-2})	530	765	588	656	739	633
Grain Length (mm)				9	9	9
Grain Width (mm)				2.6	3	3
Grain Thickness (mm)						2.07
Number of Grains/per Tiller						182

domain signal collected from the scatterometer system was converted to Power Spectrum Density to provide power information. It was then transformed into backscattering coefficient, σ° using a standard radar equation and simple averaging was performed [18]. Figure 3 shows the temporal variation of σ° of the rice crop at C-Band with various incident angles starting at 35th day of rice growth due to heavy rains on earlier stage of the growth. Each point of the graph represents an average of 20 measurements.

At HH polarization, all incident except 10° , the backscattering coefficient typically shows increasing behavior at the tillering stage, and then it decreases somewhat and increases again during reproductive stage where the panicles are formed and the plants flower. This is most probably due to the increasing scattering return as the wave interact with water and the vertical leaves of the plant particularly at the incident angle of 10° . Finally, the backscattering coefficient decreases again when the ripening stage occurs. At this point, the moisture content of the plants decreases, and the color of the plants changes from green to yellow. The curves shown in the Figure 3 are arbitrary fifth-order polynomial fits. The two peaks of the σ° of the rice crops can be observed at the end of tillering stage at about 40 days and at the end of the reproductive stage at about 80 days. This phenomenon is in contrast to the results of the rice crop measurement using X-band scatterometer [17], where



Figure 2. Rice field at Sungai Burung, Selangor, Malaysia.

σ° shows fourth-order polynomial behaviour with only single peak of σ° occurs at the end of tillering stage. The dual-peak characteristics observed in the backscattering curve in C-band is interesting where it occurs around the heading stage. The same characteristics have also been found in Ku-band [30]. This fifth-order polynomial behaviour can be an advantage for rice growth monitoring application as the additional information can be further analyzed for yield prediction. The backscattering coefficient of VV polarization at the incident angle of 10 remains consistently higher than the other polarizations. This is because the scatterometer is able to measure the radar return from the vertical stem at this angle.

Figure 4 shows the angular response of σ° of the rice crop growth. The backscattering coefficient at VV-polarization is higher than at other polarizations. This is due to the physical structure of the rice plant which consists of mainly short vertical leaves and stems that contribute to surface backscattering at VV polarization particularly during the early rice growth stages.

The dominant backscattering mechanism shifted to the volume backscattering mechanism for VV and HH polarization at the reproductive stage, thus show comparing backscattering value of VV and HH polarizations. Generally, it is shown that the cross-polarization values decrease at higher incident angles.

When the rice plants reach the ripening stage, it is observed that the total backscattering coefficient decreases slightly due to the decrease in stem and leaf densities. Although the densities of the grains

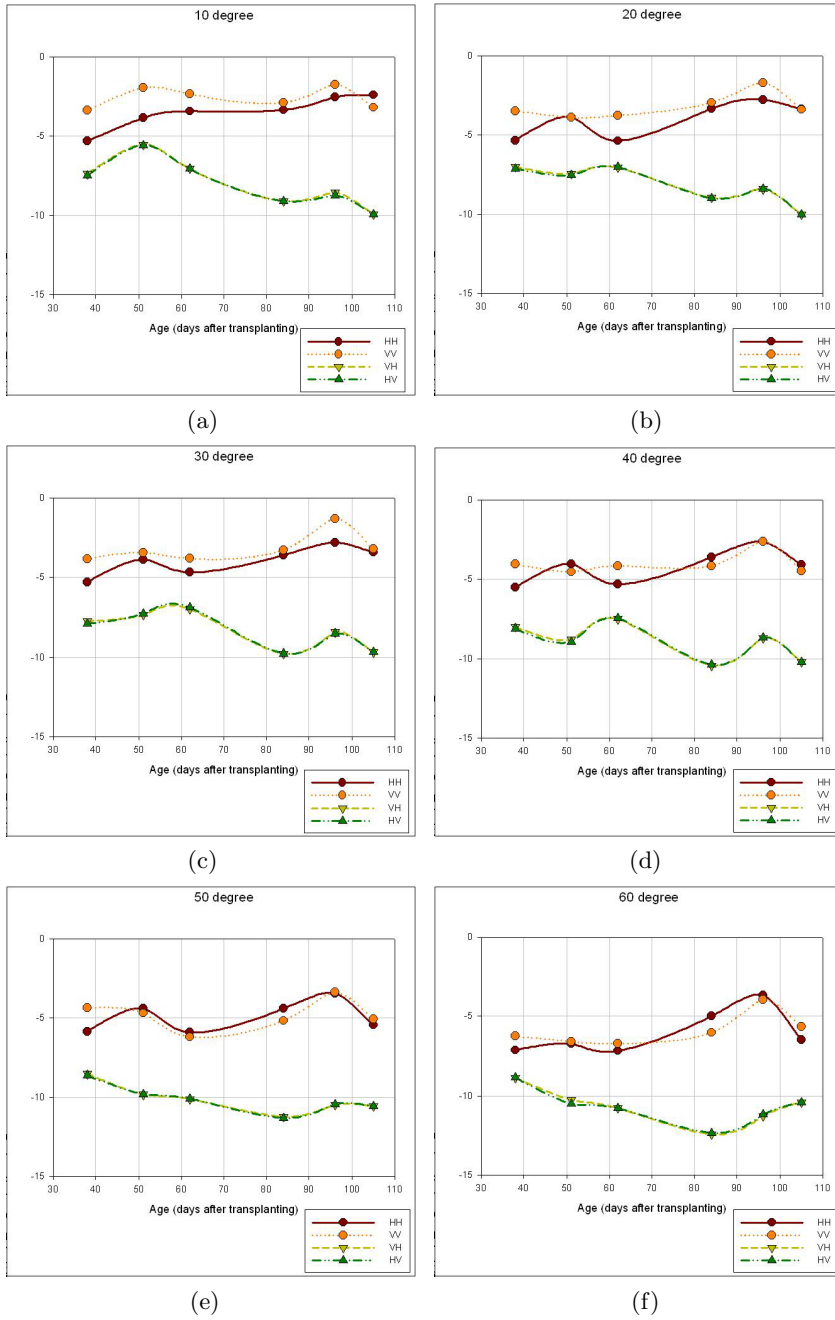


Figure 3. Temporal variation of σ^o at incident angle of (a) 10° , (b) 20° , (c) 30° , (d) 40° , (e) 50° and (f) 60° .

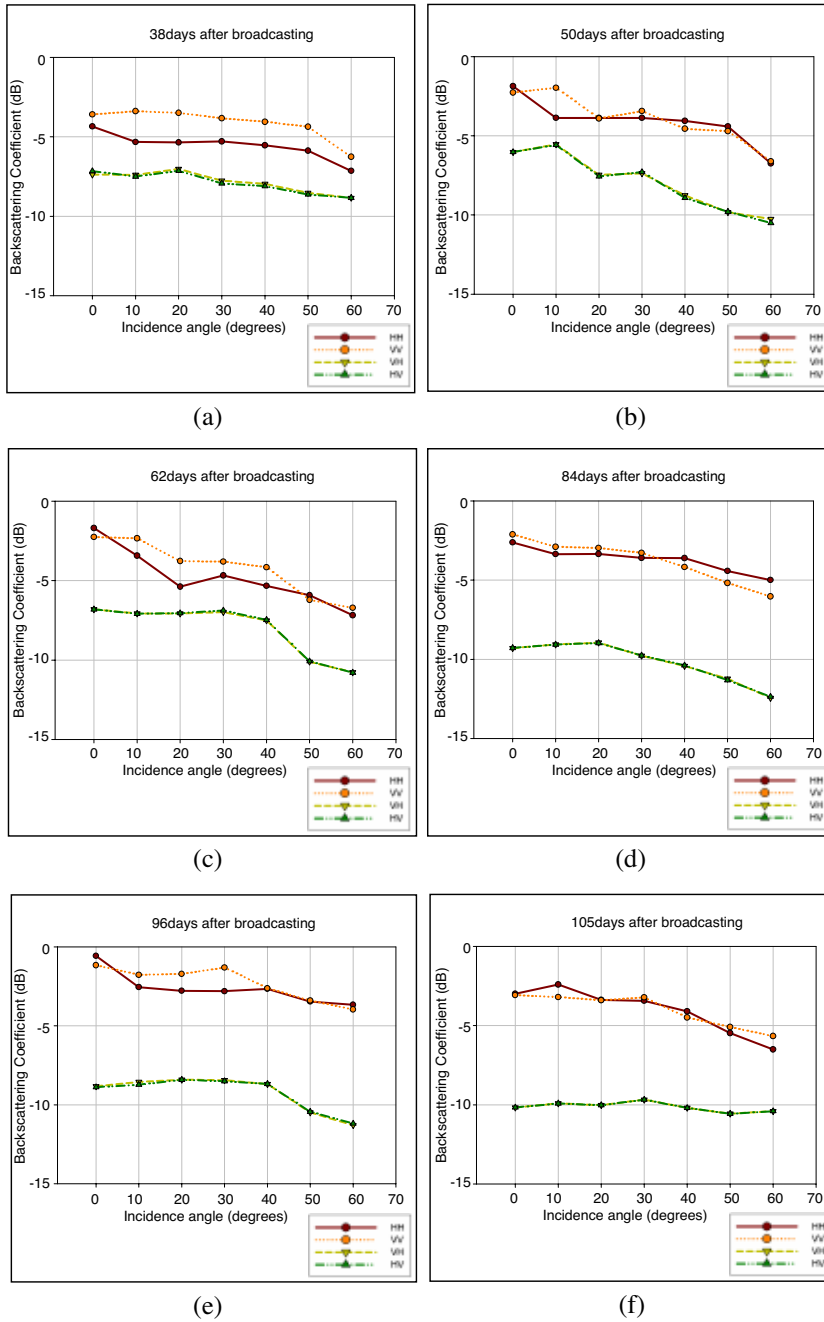


Figure 4. Angular response of σ° on (a) 38 days, (b) 50 days, (c) 62 days, (d) 84 days, (e) 96 days and (f) 105 days after transplanting.

increase at this stage of the rice growth, the stems remain the dominant contributor to the total backscattering coefficient for all polarizations. The volume backscattering for the grains remains relatively constant over all incident angles and it provides a smoothing effect on the total backscattering coefficient since the physical structure of the grains is uniformly distributed over all angles of orientation [1].

The cross-polarized backscattering coefficient is found to be decreasing with rice crop age partly because of the organized growth of the rice, causing more influence on the co-polarized signal than cross-polarized signal. Although erratic, the coefficient is decreased in a narrow margin.

4. CONCLUSIONS

An advanced automatic polarimetric scatterometer was used to investigate the multiple temporal characteristics and the monostatic angular behaviour for monitoring the different rice growth stages. HH, VV, HV and VH polarization were successfully measured with temporal variation of σ° from 0° to 60° . It is also interesting to find out that the pattern of the backscattering coefficient throughout the rice growth season is represented in fifth-order polynomials, of which similar to the finding by Inoue [31]. The measurement results showed the trend for the growth of rice crop with a temporal record of backscattering returns that would be suitable for further theoretical analysis. Theoretical modeling work is, however, in progress and the comparison results of the measured and the theoretical modeling will definitely allow more quantitative assessment of the rice growth monitoring application.

ACKNOWLEDGMENT

The authors would like to acknowledge the support of the Malaysian Remote Sensing Agency (MACRES) for the national collaboration with Multimedia University and to thank R. Zainol of the Malaysian Agricultural Department, Kuala Selangor, for his assistance in the measurement of ground truth.

REFERENCES

1. Koay, J. Y., C. P. Tan, K. S. Lim, S. Bahari, H. T. Ewe, H. T. Chuah, and J. A. Kong, "Paddy fields as electrically dense media: Theoretical modeling and measurement comparisons,"

- IEEE Transactions on Geoscience and Remote Sensing*, Vol. 45, No. 9, 2837–2849, 2007.
2. Koay, J. Y., C. P. Tan, H. T. Ewe, H. T. Chuah, and S. Bahari, “Theoretical modeling and measurement comparison of season-long rice field monitoring,” *PIERS Online*, Vol. 1, No. 1, 25–28, Hangzhou, China, 2005.
 3. Lim, K. S., C. P. Tan, J. Y. Koay, V. C. Koo, H. T. Ewe, Y. C. Lo, and A. Ali, “Multitemporal C-band radar measurement on rice fields,” *PIERS Online*, Vol. 3, No. 1, 44–47, Beijing, China, 2007.
 4. Tan, C. P., J. Y. Koay, K. S. Lim, H. T. Ewe, and H. T. Chuah, “Classification of multi-temporal SAR images for rice crops using combined entropy decomposition and support vector machine technique,” *Progress In Electromagnetics Research*, PIER 71, 19–39, 2007.
 5. De Matthaeis, P. and R. H. Lang, “Microwave scattering models for cylindrical vegetation components,” *Progress In Electromagnetics Research*, PIER 55, 307–333, 2005.
 6. Huang, E. X. and A. K. Fung, “Electromagnetic wave scattering from vegetation with odd-pinnate compound leaves,” *Journal of Electromagnetic Waves and Applications*, Vol. 19, No. 2, 231–244, 2005.
 7. Picard, G. and T. Le Toan, “A multiple scattering model for C-band backscatter of wheat canopies,” *Journal of Electromagnetic Waves and Applications*, Vol. 16, No. 10, 1447–1466, 2002.
 8. Rakotoarivony, L., O. Taconet, D. Vidal-Madjar, P. Bellemain, and M. Benallegue, “Radar backscattering over agricultural bare soils,” *Journal of Electromagnetic Waves and Applications*, Vol. 10, No. 2, 187–209, 1996.
 9. Nghiem, S. V., T. Le Toan, J. A. Kong, H. C. Han, and M. Borgeaud, “Layer model with random spheroidal scatterers for remote sensing of vegetation canopy,” *Journal of Electromagnetic Waves and Applications*, Vol. 7, No. 1, 49–75, 1993.
 10. Vecchia, A. D., L. Guerriero, I. Bruni, and P. Ferrazzoli, “Hollow cylinder microwave model for stems,” *Journal of Electromagnetic Waves and Applications*, Vol. 20, No. 3, 301–318, 2006.
 11. Blaunstein, N., D. Censor, D. Katz, A. Freedman, and I. Matityahu, “Radio propagation in rural residential areas with vegetation,” *Journal of Electromagnetic Waves and Applications*, Vol. 17, No. 7, 1039–1041, 2003.
 12. Alejandro, M., I. Chenerie, F. Baup, E. Mougin, and K. Sarabandi, “Angular normalization of ENVISAT ASAR data

- over sahelian grassland using a coherent scattering model,” *PIERS Online*, Vol. 2, No. 1, 94–98, 2006.
13. Zoughi, R., L. K. Wu, and R. K. Moore, “Identification of major backscattering sources in trees and shrubs at 10 GHz,” *Remote Sensing Environment*, Vol. 19, No. 3, 269–290, 1986.
 14. Wu, L. K., R. K. Moore, R. Zoughi, A. Afifi, and F. T. Ulaby, “Preliminary results on the determination of the sources of scattering from vegetation canopies at 10 GHz,” *International Journal of Remote Sensing*, Vol. 6, No. 2, 299–313, 1985.
 15. Paris, J. F., “Active microwave properties of vegetation,” *Fund. Remote Sensing Sci. Res. Program, 1985 Summary Report of the Scene Radiation and Atmos. Effects Characterization Project*, D. Deering (ed.), 148–154, NASA TM 86234, M.I.T., Cambridge, MA, 1985.
 16. Paris, J. F., “Characterization of cultural deciduous trees, grapes, and irrigated crops with radar and optical remote sensing,” *Ann. Rep., Microwave-optical Characterization of Vegetation with Remote Sensing Project*, NASA Lyndon B. Johnson Space Center, Houston, TX, 1985.
 17. Paris, J. F., “Radar scatterometer probing of thick vegetation canopies,” *International Geoscience Remote Sensing Symposium*, Vol. 1, 161–163, 1985.
 18. Pitts, D. E., G. D. Badhwar, and E. Reyna, “Estimation of biophysical properties of forest canopies through inversion of microwave scatterometer data,” *International Geoscience Remote Sensing Symposium*, Vol. 1, 313–320, 1985.
 19. Wu, S. T., “A preliminary report on the measurements of forest canopies with C-band radar scatterometer at NASA/NSTL,” *International Geoscience Remote Sensing Symposium*, Vol. 2, 168–173, 1985.
 20. Lopez-Sanchez, J. M., J. Fortuny-Guasch, S. R. Cloude, and A. J. Sieber, “Indoor polarimetric radar measurements on vegetation samples at L, S, C and X band,” *Journal of Electromagnetic Waves and Applications*, Vol. 14, No. 2, 205–231, 2000.
 21. Ferrazzoli, P., L. Guerriero, and D. Solimini, “Simulating bistatic scatter from surfaces covered with vegetation,” *Journal of Electromagnetic Waves and Applications*, Vol. 14, No. 2, 233–248, 2000.
 22. Ferrazzoli, P. and L. Guerriero, “Emissivity of vegetation: theory and computational aspects,” *Journal of Electromagnetic Waves and Applications*, Vol. 10, No. 5, 609–628, 1996.

23. De Carolis, G., F. Mattia, G. Pasquariello, F. Posa, and P. Smacchia, "X-band SAR and scatterometer data inversion based on geometrical optics model and Kalman filter approach," *Journal of Electromagnetic Waves and Applications*, Vol. 8, No. 8, 1017–1039, 1994.
24. Chuah, H. T., "An artificial neural network for inversion of vegetation parameters from radar backscatter coefficients," *Journal of Electromagnetic Waves and Applications*, Vol. 7, No. 8, 1075–1092, 1993.
25. Thuy, L. T., H. Laur, E. Mougin, and A. Lopes, "Multitemporal and dual-polarization observations of agricultural vegetation covers by X-band SAR images," *IEEE Transactions on Geoscience and Remote Sensing*, Vol. 27, 709–717, 1989.
26. Thuy, L. T., F. Ribbes, L. F. Wang, N. Floury, K. H. Ding, J. A. Kong, M. Fujita, and T. Kurosu, "Rice crop mapping and monitoring using ERS-1 data based on experiment and modeling results," *IEEE Transactions on Geoscience and Remote Sensing*, Vol. 35, 41–56, 1997.
27. Kurosu, T., M. Fujita, and K. Chiba, "Monitoring of rice crop growth from space using ERS1 C-band SAR," *IEEE Transactions on Geoscience and Remote Sensing*, Vol. 33, 1092–1096, 1995.
28. Kim, S. B., B. W. Kim, Y. K. Kong, and Y. S. Kim, "Radar backscattering measurements of rice crop using X-band scatterometer," *IEEE Transactions on Geoscience and Remote Sensing*, Vol. 38, 1467–1471, 2000.
29. Koo, V. C., B. K. Chung, and H. T. Chuah, "Development of a ground-based radar for scattering measurements," *IEEE Antennas and Propagation Magazine*, Vol. 45, No. 2, 36–42, 2003.
30. Oza, S. R. and J. S. Parihar, "Evaluation of Ku-band QuikSCAT scatterometer data for rice crop growth stage assessment," *International Journal of Remote Sensing*, Vol. 28, No. 16, 3447–3456, 2007.
31. Inoue, Y., T. Kurosu, H. Maeno, S. Uratsuka, T. Kozu, K. Dabrowska-Zielinska, and J. Qi, "Season-long daily measurements of multifrequency (Ka, Ku, X, C, and L) and full polarization backscattering signatures over paddy rice field and their relationship with biological variables," *Remote Sensing of Environment*, Vol. 81, No. 2–3, 194–204, 2002.